J. Fluid Mech. (1989), *vol.* 199, *pp.* 155–176
Printed in Great Britain

Linearized dynamics of spherical bubble clouds

By LUCA D'AGOSTINO AND CHRISTOPHER E. BRENNEN
California Institute of Technology, Pasadena, CA 91125, USA

(Received 22 December 1987 and in revised form 27 May 1988)

The present work investigates the dynamics of the one-dimensional, unsteady flow of a spherical bubble cloud subject to harmonic far-field pressure excitation. Bubble dynamics effects and energy dissipation due to viscosity, heat transfer, liquid compressibility and relative motion of the two phases are included. The equations of motion for the average flow and the bubble radius are linearized and a closed-form solution is obtained. The results are then generalized by means of Fourier synthesis to the case of arbitrary far-field pressure excitation. The flow displays various regimes (sub-resonant, trans-resonant and super-resonant) with different properties depending on the value of the relevant flow parameters. Examples are discussed in order to show the effects of the inclusion of the various energy dissipation mechanisms. Finally the results for the case of Gaussian-shaped far-field pressure change are presented and the most important limitations of the theory are briefly discussed. The simple linearized dynamical analysis developed so far clearly demonstrates the importance of the complex phenomena connected to the interaction of the dynamics of the bubbles with the flow and provides an introduction to the more realistic study of the same flows with nonlinear bubble dynamics.

1. Introduction

This paper illustrates part of our current research on the role played by the dynamics of bubble volume changes in the fluid mechanics of bubbly or cavitating flows. It represents the natural extension of our previous work on the dynamics of steady two-dimensional bubbly flows over slender profiles (d'Agostino, Brennen & Acosta 1988). Specifically, it studies the effects of the inclusion of bubble dynamic response in one-dimensional unsteady flows of spherical bubble clouds subject to far-field pressure perturbation.

Among the practical objectives of this study is a better understanding of the global effects of many bubbles on the dynamics and, in particular, on the acoustical behaviour of bubbly and cavitating flows. Traditionally the acoustical properties of bubbly cavitating flows have been analysed and interpreted on the basis of single-bubble dynamics as the colletive result of the simultaneous but independent contributions due to the presence of a wide spectrum of bubbles. The interactive effects that the bubble volume changes can have on the pressure distribution (and therefore on the flow velocity field) were neglected, thus preventing the analysis of any large-scale internal motion in the bubbly region of the flow. The traditional approach may be adequate when the bubble concentration is extremely low and only occasional bubbles occur, but it clearly loses validity when the bubble concentration becomes larger and the possibility of global motion in the bubbly mixture arises. In this case significant alterations will occur in the pressure distribution and therefore in the dynamic behaviour of the bubbly flow. For example, the optical observations of travelling bubble cavitation on Schiebe headforms in water tunnel tests by Marboe,

Billet & Thompson (1986) and the simultaneous measurements of the noise spectrum displayed the tendency of the noise spectrum to shift towards lower frequencies than expected from single-bubble dynamics considerations. Marboe and his co-workers suggested the occurrence of asymmetric bubble collapse as a possible cause of this phenomenon. In view of our current results global bubble interaction effects in the cavitation region when a sufficient concentration of bubbles is present are another possible explanation of the observed downward shift of the cavitation noise spectrum. Similar recent experimental results by Arakeri & Shanmuganathan (1985) and M. Billet (1986, personal communication) have also helped identify bubble interactions in cavitating flows as a likely source of the observed discrepancies. The main purpose of this research is to provide some physical interpretation of the origin of these alterations. Despite the extensive linearizations inherent in the analysis we are confident that the results convey some qualitative understanding of the dynamic and acoustical properties of real bubbly flows.

The last few decades have seen extensive research on the dynamics of bubbly flows (van Wijngaarden 1968, 1972; Stewart & Wendroff 1984). Early studies based on space-averaged equations for the mixture in the absence of relative motion between the two phases (Tangren, Dodge & Seifert 1949) did not consider bubble dynamic effects. This approach simply leads to an equivalent compressible homogeneous medium. In a classic paper Foldy (1945) accounted for the dynamics of individual bubbles by treating them as randomly distributed point scatterers. Assuming that the system is ergodic, the collective effect of bubble dynamic response on the flow is then obtained by taking the ensemble average over all possible configurations. Later, more general equivalent flow models of dispersed two-phase mixtures, which include the effects of bubble dynamics, liquid compressibility and relative motion, have been developed by ensemble, volume (Biesheuvel & van Wijngaarden 1984) or time (Ishii 1975) averaging of the conservation equations for each separate phase. These models have been successfully applied to describe the propagation of both infinitesimal and finite-amplitude one-dimensional disturbances through liquids containing small gas bubbles (Carstensen & Foldy 1947; Fox, Curley & Larson 1955; Macpherson 1957; Silberman 1957; Noordzij 1973; Noordzij & van Wijngaarden 1974).

A natural way to account for the effects of bubble dynamics and slip velocity between the two phases is to include the Rayleigh–Plesset and the relative motion equations in the space-averaged equations. However, because of their complexity, there are few reported examples of the application to specific flow geometries of the space-averaged equations which include the effects of bubble response. Recently Mørch (1980, 1981), Chahine (1982*a*, *b*), and others have focused their attention on the dynamics of a cloud or cluster of cavitating bubbles and have expanded on the work of van Wijngaarden (1964). Unfortunately, there appear to be a number of inconsistencies in this recent work which will require further study before a coherent body of knowledge on the dynamics of clouds of bubbles is established. For example, the early work of Chahine (1982*a*) does not account for the large-scale effects that the bubble volume changes have on the velocity field and therefore on the pressure experienced by each individual bubbles, though in a later paper Chahine (1982*b*) does begin to consider these global interactions. On the other hand, Mørch and his co-workers (1980, 1981, 1982) have visualized the collapse of a cloud of cavitating bubbles as involving the inward propagation of a shock wave: it is assumed that the bubbles collapse completely when they encounter the shock. This implies the virtual absence of non-condensable gas in the bubbles and the predominance of vapour. Yet in these circumstances the mixture in the cloud will not have any real sonic speed.

As implied by a negative left-hand side of equation (13), the fluid motion equations for the mixture would be elliptic not hyperbolic and hence shock-wave solutions seem inappropriate. A discussion of the nature of the characteristics of spherical cavity clouds is contained in Pylkkänen (1986) for various bubbly flow models containing four, five and six independent variables.

In the present programme we focused our attention on one-dimensional steady flows or two-dimensional time-dependent flows. In an earlier publication (d'Agostino *et al.* 1988) and two previous notes (d'Agostino & Brennen 1983; d'Agostino, Brennen & Acosta 1984) we considered the two-dimensional steady flow of a bubbly liquid over wave-shaped surfaces and the undamped linearized dynamics of a spherical cloud of bubbles subject to an harmonic pressure field. The results clearly show that the fluid motion can be critically controlled by bubble dynamic effects. Specifically, the dominating phenomenon consists of the combined response of the bubbles to the pressure in the surrounding liquid, which results in volume changes leading to a global accelerating velocity field. Associated with this velocity field is a pressure gradient which in turn determines the pressure encountered by each individual bubble in the mixture. Furthermore, it can be shown that such global interactions usually dominate any local pressure perturbations experienced by one bubble due to the growth or collapse of a neighbour (see §5). In the present work the same approach, generalized with the inclusion of energy dissipation in the dynamics of the bubbles, liquid compressibility effects and relative motion between the two phases, is first applied to the time-dependent one-dimensional radial flow in a spherical bubble cloud subject to harmonic far-field pressure perturbations and then is extended to the case of small but arbitrary pressure excitation.

During the preparation of this paper, the bubble-cloud flow problem has been independently addressed by Omta (1987) using a similar approach. Omta linearized the Biesheuvel–van Wijngaarden homogeneous flow equations for a bubbly mixture (Biesheuvel & van Wijngaarden 1984) and derived an analytical solution to the flow in a spherical bubble cloud. In his work a number of simplifying assumptions have been introduced with respect to the present analysis. With a slight inconsistency, Omta neglected viscosity and liquid compressibility (and therefore their contributions to damping) in the bubble dynamics, but retained them when considering the relative motion of the two phases and the propagation of pressure disturbances in the liquid. Surface tension has also been neglected and relative motion does not affect the solution explicitely, since in Omta's derivation the slip-velocity problem is fully decoupled from the cloud dynamics. Thus thermal damping is in practice the only dissipation mechanism accounted for. On the other hand, the above effects are included in the present theory and therefore their relative importance can be easily assessed. Although viscous and acoustic damping in the bubble dynamics and surface-tension effects can be important in small bubbles at high excitation frequencies (as indicated by Plesset & Prosperetti 1977 and confirmed here), the two treatments lead to virtually the same main conclusions on the general characteristics of the flow in the bubble cloud. Despite all its intrinsic limitations, the following linear analysis indicates some of the fundamental phenomena involved and represents a useful basis for the study of such flows with nonlinear bubble dynamics (which we intend to discuss in a later publication).

2. Basic equations

Following the same approach previously indicated in our earlier works (d'Agostino & Brennen 1983; d'Agostino *et al.* 1984, 1988), several simplifying assumptions are introduced to obtain a soluble set of equations which still reflects the effects of bubble dynamic response. The relative motion of the two phases is initially neglected. The liquid is assumed inviscid and incompressible, with a density ρ and constant concentration β of bubbles per unit liquid volume. Also, the mass of the dispersed phase and all damping mechanisms in the dynamics of the bubbles are initially neglected. The effects introduced by the inclusion of the heat transfer and relative motion between the phases as well as of the viscosity and compressibility of the liquid on the energy dissipation in the flow will be considered later. Then, if external body forces are unimportant, the velocity $\boldsymbol{u}(\boldsymbol{x}, t)$ and the pressure $p(\boldsymbol{x}, t)$ (defined as the corresponding quantities in the liquid in the absence of local perturbations due to any neighbouring bubbles), satisfy the continuity and momentum equations in the form

$$\nabla \cdot \boldsymbol{u} = \frac{\beta}{1+\beta\tau}\frac{\mathrm{D}\tau}{\mathrm{D}t}, \tag{1}$$

$$\rho\frac{\mathrm{D}\boldsymbol{u}}{\mathrm{D}t} = -(1+\beta\tau)\nabla p, \tag{2}$$

where $\mathrm{D}/\mathrm{D}t$ indicates the Lagrangian derivative, $\tau(\boldsymbol{x}, t)$ is the individual bubble volume and β is related to the void fraction α by $\beta\tau = \alpha/(1-\alpha)$. Finally, under the additional hypothesis that the bubbles remain spherical, it follows that $\tau = 4\pi R^3/3$, with the bubble radius $R(\boldsymbol{x}, t)$ determined by the Rayleigh–Plesset equation (Plesset & Prosperetti 1977; Knapp, Daily & Hammit 1970):

$$\frac{p_{\mathrm{B}}-p}{\rho} = R\frac{\mathrm{D}^2R}{\mathrm{D}t^2}+\frac{3}{2}\left(\frac{\mathrm{D}R}{\mathrm{D}t}\right)^2+\frac{2S}{\rho R}. \tag{3}$$

Here S is the surface tension and p_{B} is the bubble internal pressure, which consists of the partial pressures of the vapour p_{V} and non-condensable gas p_{G}. Neglecting thermal and mass diffusion effects within the bubbles, p_{V} is assumed constant and p_{G} is expressed by the polytropic relation of index q: $p_{\mathrm{G}} = p_{\mathrm{G}_0}(R/R_0)^{3q}$, where p_{G_0} is the gas partial pressure at the reference radius R_0. Mass diffusion effects and other non-stationary phenomena are not, of course, included in the present theory. The determination of the polytropic index q requires the solution of the energy transfer problem across the bubble surface, as shown later in § 3. For now, its value remains undetermined in the range from 1, in the isothermal limit, to γ, the ratio of the specific heats of the non-condensable gas in the bubbles, which corresponds to isentropic conditions.

Equations (1), (2) and (3), together with suitable boundary conditions, represent in theory a complete system of equations for $\boldsymbol{u}(\boldsymbol{x}, t)$, $p(\boldsymbol{x}, t)$, and $\tau(\boldsymbol{x}, t)$. However, in practice their highly nonlinear nature requires further simplifications for a closed-form solution to be attained even for very simple flows.

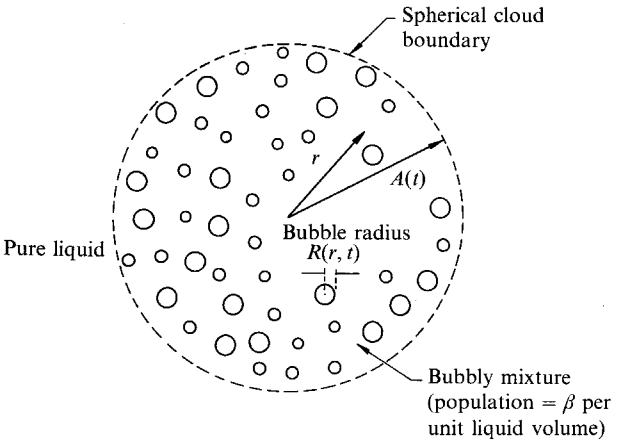

FIGURE 1. Schematic of a spherical cloud of bubbles.

3. Dynamics of spherical bubble clouds

3.1. *Undamped case – harmonic excitation*

We consider first the problem of a one-dimensional inviscid flow of a spherical cloud of bubbles in an unbounded liquid at rest at infinity, as shown in figure 1. Let the perturbation of the far-field pressure be defined in complex notation by the equation: $p_\infty(t) = p_0[1+\epsilon \exp(i\omega t)]$ with $\epsilon \ll 1$ and let the subscript 0 indicate the unperturbed conditions corresponding to $\epsilon = 0$. Then, assuming for simplicity that all the bubbles have the same radius R_0, the undisturbed pressure in the liquid is

$$p_0 = p_{G_0} + p_v - \frac{2S}{R_0}. \tag{4}$$

We limit our analysis to the case of uniform and relatively low void fraction so that the mean-flow velocity is small and purely radial, with component $u(r, t)$. Then (1), (2) and (3) reduce to

$$\frac{1}{r^2}\frac{\partial}{\partial r}(r^2 u) = (1-\alpha_0)\beta\frac{\partial \tau}{\partial t}, \tag{5}$$

$$(1-\alpha_0)\rho\frac{\partial u}{\partial t} = -\frac{\partial p}{\partial r}, \tag{6}$$

$$p = p_v + p_{G_0}\left(\frac{R_0}{R}\right)^{3q} - \frac{2S}{R} - \rho\left[R\frac{\partial^2 R}{\partial t^2} + \frac{3}{2}\left(\frac{\partial R}{\partial t}\right)^2\right]. \tag{7}$$

Finally, eliminating u from (5) and (6) and using (7), one obtains the following equation for $R(r, t)$:

$$\frac{1}{r^2}\frac{\partial}{\partial r}\left\{r^2\frac{\partial}{\partial r}\left[R\frac{\partial^2 R}{\partial t^2} + \frac{3}{2}\left(\frac{\partial R}{\partial t}\right)^2 - \frac{p_{G_0}}{\rho}\left(\frac{R_0}{R}\right)^{3q} + \frac{2S}{\rho R}\right]\right\} = \frac{\alpha_0(1-\alpha_0)\rho}{R_0^3}\frac{\partial^2 R^3}{\partial t^2}; \quad r \leqslant A(t) \tag{8}$$

inside the cloud. For the incompressible single-phase flow outside the cloud,

$$u(r, t) = \frac{C(t)}{r^2}; \quad p(r, t) = p_\infty(t) + \frac{\rho}{r^2}\frac{\mathrm{d}C(t)}{\mathrm{d}t} + O(C^2(t)); \quad r \geqslant A(t), \tag{9}$$

where $C(t)$ is of perturbation order in low-void-fraction flows. It follows that the continuity of $p(r, t)$ and $u(r, t)$ at the interface between the cloud and the pure liquid results in the following linearized boundary condition for $R(r, t)$:

$$\left(1+\frac{A_0}{1-\alpha_0}\frac{\partial}{\partial r}\right)\left\{R\frac{\partial^2 R}{\partial t^2}+\frac{3}{2}\left(\frac{\partial R}{\partial t}\right)^2-\frac{p_v}{\rho}-\frac{p_{G_0}}{\rho}\left(\frac{R_0}{R}\right)^{3q}+\frac{2S}{\rho R}\right\}_{r=A_0}=-\frac{p_\infty(t)}{\rho}, \tag{10}$$

where A_0 is the unperturbed radius of the bubble cloud. In addition the solution is required to be periodic in time with frequency ω.

The nonlinear equations (8) and (10) do not have any known analytical solution. In order to investigate their fundamental behaviour, we therefore examine the linearized form of these equations for small changes of the bubble radius

$$R(r, t) = R_0[1+\varphi(r, t)],$$

where $|\varphi(r, t)| \ll 1$. Then, to the first order in φ,

$$\frac{1}{r^2}\frac{\partial}{\partial r}\left(r^2\frac{\partial}{\partial r}\right)\left(\frac{1}{\omega_B^2}\frac{\partial^2\varphi}{\partial t^2}+\varphi\right)-\frac{1}{c_m^2}\frac{\partial^2\varphi}{\partial t^2}=0, \tag{11}$$

$$\left(1+\frac{A_0}{1-\alpha_0}\frac{\partial}{\partial r}\right)\left(\frac{1}{\omega_B^2}\frac{\partial^2\varphi}{\partial t^2}+\varphi\right)_{r=A_0}=\frac{p_0-p_\infty(t)}{\rho R_0^2\omega_B^2}, \tag{12}$$

where ω_B is the natural frequency of oscillation of a single bubble at isothermal conditions in an unbounded liquid (Plesset & Prosperetti 1977; Knapp *et al.* 1970),

$$\omega_B^2=\frac{3p_{G_0}}{\rho R_0^2}-\frac{2S}{\rho R_0^3}; \tag{13}$$

and

$$c_m^2=\frac{\omega_B^2 R_0^2}{3\alpha_0(1-\alpha_0)} \tag{14}$$

is the low-frequency sound speed in the absence of dispersive effects. If the bubbles are in stable equilibrium in their mean or unperturbed state, then $3p_{G_0} > 2S/R_0$ and both ω_B and c_m are real.

When surface tension and vapour pressure are neglected (14) reduces to the well-known expression of the low-frequency sound speed for a homogeneous mixture (van Wijngaarden 1980). On the other hand, (11) is the familiar one-dimensional wave equation (van Wijngaarden 1980) in spherical coordinates for the radial propagation of acoustical disturbances in a bubbly medium in the absence of energy dissipation. The corresponding dispersion equation for spherical waves of the form $[\exp i(kr+\omega t)]/r$ is

$$\frac{1}{c_{m\omega}^2}=\frac{k^2}{\omega^2}=\frac{1}{c_m^2}\left(\frac{\omega_B^2}{\omega_B^2-\omega^2}\right), \tag{15}$$

where $c_{m\omega}$ is the speed of propagation of an harmonic disturbance of angular frequency ω. The present derivation of (11), however, has the advantage of explicitly formulating the boundary-value problem (8) and (10) which has to be addressed when the hypothesis of linearized bubble dynamics is relaxed.

The solution of (11) in the domain $r \leqslant A_0$ for the case of a spherical bubble cloud subject to harmonic far-field pressure excitation is

$$\varphi(r, t)=-\epsilon\frac{p_0(1-\alpha_0)/\rho R_0^2}{\omega_B^2-\omega^2}\left(\frac{1}{\cos kA_0-\alpha_0\sin(kA_0)/kA_0}\right)\frac{\sin kr}{kr}e^{i\omega t}. \tag{16}$$

Here k is the principal square root (with non-negative real and imaginary parts) of k^2 as expressed by (15). The other possible solution involving $\cos(kr)/kr$ has been eliminated since at the cloud centre $\varphi(r, t)$ must be finite. Therefore inside the cloud $(r \leqslant A_0)$

$$R(r, t) = R_0 - R_0 \epsilon \frac{p_0(1-\alpha_0)/\rho R_0^2}{\omega_B^2 - \omega^2} \left(\frac{1}{\cos kA_0 - \alpha_0 \sin(kA_0)/kA_0} \right) \frac{\sin kr}{kr} e^{i\omega t}, \tag{17}$$

$$p(r, t) = p_0 + p_0 \epsilon \frac{1-\alpha_0}{\cos kA_0 - \alpha_0 \sin(kA_0)/kA_0} \left(\frac{\sin kr}{kr} \right) e^{i\omega t}, \tag{18}$$

$$u(r, t) = i\epsilon \frac{p_0/\rho\omega r}{\cos kA_0 - \alpha_0 \sin(kA_0)/kA_0} \left(\cos kr - \frac{\sin kr}{kr} \right) e^{i\omega t}, \tag{19}$$

$$\frac{\partial u}{\partial t}(r, t) = -\epsilon \frac{p_0/\rho r}{\cos kA_0 - \alpha_0 \sin(kA_0)/kA_0} \left(\cos kr - \frac{\sin kr}{kr} \right) e^{i\omega t}. \tag{20}$$

3.2. *Damped case – harmonic excitation*

Energy dissipation in bubbly flows naturally originates from various sources such as viscosity, heat and mass transfer in the two phases and sound radiation from the bubbles. In particular, viscous effects occur, owing to the interaction of the flow with the boundaries, to the relative velocity of the two phases, or as a consequence of the motion associated with the volume changes of the bubbles. In the further development of the theory of bubbly clouds with harmonic far-field pressure excitation we consider the energy dissipation due to the relative motion of the two phases and the most important forms of damping which occur in the dynamics of the bubbles due to thermal effects and to the viscosity and compressibility of the liquid.

We therefore address the problem of the simultaneous solution of the fluid dynamic equations for the two phases with the relevant interaction terms. Let $\boldsymbol{u}(\boldsymbol{x}, t)$ be the velocity of the liquid, $\boldsymbol{v}(\boldsymbol{x}, t)$ the velocity of the bubbles and $\boldsymbol{w}(\boldsymbol{x}, t) = \boldsymbol{v}(\boldsymbol{x}, t) - \boldsymbol{u}(\boldsymbol{x}, t)$ the relative velocity of the two phases. The effects of the liquid compressibility are included by introducing the speed of sound in the liquid $c = (\mathrm{d}p/\mathrm{d}\rho)^{\frac{1}{2}}$ and rewriting the liquid continuity equation (1) as

$$\nabla \cdot \boldsymbol{u} = \frac{1}{1+\beta\tau} \frac{\mathrm{D}_u(\beta\tau)}{\mathrm{D}_u t} - \frac{1}{\rho c^2} \frac{\mathrm{D}_u p}{\mathrm{D}_u t}, \tag{21}$$

where $\mathrm{D}_u/\mathrm{D}_u t = \partial/\partial t + \boldsymbol{u} \cdot \nabla$ indicates the Lagrangian time derivative following the liquid. Note that $\beta(\boldsymbol{x}, t)$ is no longer constant owing to the effects of the relative motion. Under the additional hypothesis that no bubbles are created or destroyed, the number continuity equation gives

$$\nabla \cdot \boldsymbol{v} = \frac{1}{1+\beta\tau} \frac{\mathrm{D}_v(\beta\tau)}{\mathrm{D}_v t} - \frac{1}{\beta} \frac{\mathrm{D}_v p}{\mathrm{D}_v t}. \tag{22}$$

Here $\mathrm{D}_v/\mathrm{D}_v t = \partial/\partial t + \boldsymbol{v} \cdot \nabla$ indicates the Lagrangian time derivative following the bubbles. Furthermore, the momentum equation for the liquid phase now becomes

$$\rho \frac{\mathrm{D}_u \boldsymbol{u}}{\mathrm{D}_u t} = -(1+\beta\tau) \nabla p. \tag{23}$$

In order to account for the viscous dissipation in the bubble dynamics, the Rayleigh–Plesset equation (3) is modified as indicated by Keller *et al.* (see Prosperetti 1984):

$$\left(1-\frac{\dot{R}}{c}\right)R\ddot{R}+\frac{3\dot{R}^2}{2}\left(1-\frac{\dot{R}}{3c}\right)=\left(1+\frac{\dot{R}}{c}\right)\frac{p_R(t)+p(t+R/c)}{\rho}+\frac{R}{\rho c}\frac{\mathrm{d}p_R(t)}{\mathrm{d}t}, \tag{24}$$

where $p_R(t)$ is the liquid pressure at the bubble surface, related to the bubble internal pressure p_B (assumed uniform) by

$$p_B(t)=p_R(t)+\frac{2S}{R}+4\mu\frac{\dot{R}}{R}. \tag{25}$$

Here dots denote Lagrangian time derivatives following the bubbles and μ is the viscosity of the pure liquid. Finally, the momentum balance for the dispersed phase, as required for the closure of the problem, is given by the relative motion equation for a spherical bubble of negligible mass in a viscous liquid with Stokes' drag (Voinov 1973)

$$\frac{\rho\tau}{2}\frac{\mathrm{D}_v\boldsymbol{v}}{\mathrm{D}_v t}-\frac{\rho\tau}{2}\frac{\mathrm{D}_u\boldsymbol{u}}{\mathrm{D}_u t}+6\pi\mu R(\boldsymbol{v}-\boldsymbol{u})+\frac{\rho(\boldsymbol{v}-\boldsymbol{u})}{2}\frac{\mathrm{D}_v\tau}{\mathrm{D}_v t}-\tau\nabla p=0. \tag{26}$$

Linearization of (24) and (25) for small changes under the action of a periodic pressure perturbation $p(t)=p_0(1-\sigma\exp\mathrm{i}\omega t)$ leads to modelling each individual gas bubble as an harmonic oscillator

$$\ddot{\varphi}(t)+2\lambda\dot{\varphi}(t)+\omega_{B\omega}^2\varphi(t)=\delta\sigma\mathrm{e}^{\mathrm{i}\omega t}, \tag{27}$$

with internal pressure $p_B(t)=p_{B_0}[1-\phi\varphi(t)]$, where

$$2\lambda=\frac{4\mu}{\rho R_0^2}+\frac{\omega^2 R_0}{c}+\frac{p_{B_0}}{\rho\omega R_0^2}\mathrm{Im}\,(\phi), \tag{28}$$

$$\omega_{B\omega}^2=\mathrm{Re}\,(\phi)\frac{p_{B_0}}{\rho R_0^2}-\frac{2S}{\rho R_0^3}, \tag{29}$$

$$\delta=\frac{p_0}{\rho R_0^2}\left(1-\mathrm{i}\frac{\omega R_0}{c}\right), \tag{30}$$

$$\phi=\frac{3\gamma\theta^2}{\theta[\theta+3(\gamma-1)A_-]-\mathrm{i}3(\gamma-1)(\theta A_+-2)}, \tag{31}$$

$$A_\pm=\frac{\sinh\theta\pm\sin\theta}{\cosh\theta-\cos\theta} \tag{32}$$

and $\theta=R_0(2\omega/\chi_G)^{\frac{1}{2}}$ is the ratio of the bubble radius to the bubble thermal diffusion length. The three terms of the effective damping coefficient λ respectively represent the contributions of the viscous, acoustical and thermal dissipation, while $\omega_{B\omega}$ is the effective natural frequency of the oscillator when excited at frequency ω. Finally, the complex parameters δ, ϕ and σ account for the magnitude ratio and phase difference between the related quantities. In particular, $\mathrm{Re}(\phi)/3$ can be interpreted as the effective polytropic exponent of the gas in the bubble and respectively tends to 1 and γ in the isothermal and isentropic limts for $\omega\to 0$ and $\omega\to+\infty$ (Prosperetti 1984).

Introducing the radial component of the relative velocity $w(r,t)=v(r,t)-u(r,t)$

and using the same approach as previously followed for the undamped-case, equations (21), (22), (23) and (26) reduce to

$$\frac{1}{r^2}\frac{\partial}{\partial r}(r^2u) = (1-\alpha_0)\beta_0\frac{\partial\tau}{\partial t}+(1-\alpha_0)\tau_0\frac{\partial\beta}{\partial t}-\frac{1}{\rho c^2}\frac{\partial p}{\partial t}, \tag{33}$$

$$\frac{1}{r^2}\frac{\partial}{\partial r}(r^2w) = -\frac{1}{\beta_0}\frac{\partial\beta}{\partial t}+\frac{1}{\rho c^2}\frac{\partial p}{\partial t}, \tag{34}$$

$$(1-\alpha_0)\rho\frac{\partial u}{\partial t} = -\frac{\partial p}{\partial r}, \tag{35}$$

$$\frac{\partial w}{\partial t}+\left(\frac{9\nu}{R_0^2}+\frac{1}{R_0^2}\frac{\partial R^3}{\partial t}\right)w+\frac{2}{\rho}\frac{\partial p}{\partial r} = 0. \tag{36}$$

Upon the assumption of a $(2\pi/\omega)$-periodic behaviour in time, the above forms of energy dissipation can be incorporated in the theory for the linearized dynamics of bubble clouds subject to harmonic far-field pressure excitation. The previous approach leads to a generalized definition of the dispersion equation:

$$\frac{1}{c_{\mathrm{m}\omega}^2} = \frac{k^2}{\omega^2} = \left[\frac{1}{c_{\mathrm{m}}^2}\left(\frac{\omega_{\mathrm{B}}^2(1-\mathrm{i}\omega R_0/c)}{\omega_{\mathrm{B}\omega}^2-\omega^2+\mathrm{i}\omega 2\lambda}\right)+\frac{(1-\alpha_0)^2}{c^2}\right]\Big/\left(1+\frac{2\alpha_0(1-\alpha_0)}{1+9\nu/\mathrm{i}\omega R_0^2}\right), \tag{37}$$

where $c_{\mathrm{m}\omega}$ now becomes complex and $\nu = \mu/\rho$ is the kinematic viscosity of the liquid. Note that the effects of relative motion and liquid compressibility are small in flows of moderate void fraction where $\alpha \ll 1$ and $c_{\mathrm{m}\omega} \ll c$. The expressions for the bubble radius, the relative velocity and the bubble concentration per unit liquid volume now become

$$R(r,t) = R_0-R_0\epsilon\frac{p_0(1-\alpha_0)/\rho R_0^2}{\omega_{\mathrm{B}\omega}^2-\omega^2+\mathrm{i}\omega 2\lambda}\left(\frac{1-\mathrm{i}\omega R_0/c}{\cos kA_0-\alpha_0\sin(kA_0)/kA_0}\right)\frac{\sin kr}{kr}\mathrm{e}^{\mathrm{i}\omega t}, \tag{38}$$

$$w(r,t) = \mathrm{i}\epsilon\left(\frac{p_0/\rho\omega r}{\cos kA_0-\alpha_0\sin(kA_0)/kA_0}\right)\frac{2(1-\alpha_0)}{1+9\nu/\mathrm{i}\omega R_0^2}\left(\cos kr-\frac{\sin kr}{kr}\right)\mathrm{e}^{\mathrm{i}\omega t}, \tag{39}$$

$$\beta(r,t) = \beta_0+\beta_0\epsilon\frac{p_0}{\rho}\left(\frac{1}{c^2}+\frac{k^2}{\omega^2}\right)\frac{1-\alpha_0}{\cos kA_0-\alpha_0\sin(kA_0)/kA_0}\left(\frac{\sin kr}{kr}\right)\mathrm{e}^{\mathrm{i}\omega t}, \tag{40}$$

while the formal expressions (18)–(20) of the solution for the other flow quantities remain the same.

The entire flow has therefore been determined in terms of the material properties of the phases, the nature of the far-field pressure excitation and of the assigned quantities: α_0, R_0, A_0 and p_0.

3.3. *Damped case – arbitrary excitation*

Owing to the linear nature of the problem, the above solution can readily be generalized to the case of arbitrary but small far-field pressure excitation. If $p_\infty(t) = p_0[1+\eta(t)]$ and $H(\omega)$ is the Fourier transform of $\eta(t)$, such that in complex notation

$$\eta(t) = \int_0^{+\infty} H(\omega)\,\mathrm{e}^{\mathrm{i}\omega t}\,\mathrm{d}\omega, \tag{41}$$

then the linearized solution $f(r, t)$ of (11) admits the following integral representation:

$$f(r, t) = \int_0^{+\infty} H(\omega) f_\omega(r, t, \omega) \, \mathrm{d}\omega, \tag{42}$$

where $f_\omega(r, t, \omega)$ is the corresponding harmonic solution for given ω and $\epsilon = 1$. Thus, for instance, the normalized bubble radius for the case of energy dissipation is expressed by

$$\varphi(r, t) = -\int_0^{+\infty} H(\omega) \frac{p_0(1-\alpha_0)/\rho R_0^2}{\omega_{\mathrm{B}\omega}^2 - \omega^2 + \mathrm{i}\omega 2\lambda} \left(\frac{(1 - \mathrm{i}\omega R_0/c) \sin(kr)/kr}{\cos kA_0 - \alpha_0 \sin(kA_0)/kA_0} \right) \mathrm{e}^{\mathrm{i}\omega t} \, \mathrm{d}\omega, \tag{43}$$

where k, $\omega_{\mathrm{B}\omega}$ and λ are functions of the angular frequency ω.

4. Results and discussion

In this Section we consider the case of air bubbles ($\gamma = 1.4$, $\chi_{\mathrm{G}} = 0.0002\ \mathrm{m}^2/\mathrm{s}$) in water ($\rho = 1000\ \mathrm{kg/m}^3$, $\mu = 0.001\ \mathrm{Ns/m}^2$, $S = 0.0728\ \mathrm{N/m}$, $c = 1485\ \mathrm{m/s}$). The other relevant flow parameters are: $p_0 = 10^5\ \mathrm{Pa}$, $R_0 = 0.001\ \mathrm{m}$, $A_0 = 0.1\ \mathrm{m}$ and $\epsilon = 0.1$. Finally, in most cases the parameter $\omega_{\mathrm{B}}^2 A_0^2/c_{\mathrm{m}}^2 = 3\alpha_0(1-\alpha_0) A_0^2/R_0^2$ is assigned and the void fraction α_0 is determined accordingly. Also note that in the damped bubble dynamic case the normalization of the data has been carried out with respect to the bubble resonance frequency ω_{B} defined as the solution of the equation: $\omega_{\mathrm{B}} = \omega_{\mathrm{B}\omega}(\omega_{\mathrm{B}})$. This choice preserves the occurrence of bubble resonance for $\omega/\omega_{\mathrm{B}} = 1$, with the advantage of making the plots for the damped case more readily comparable to the corresponding ones in the absence of damping.

In order to identify the natural frequencies and mode shapes of the bubble cloud we now examine first the nature of the above solution in the absence of energy dissipation. From (16) note that if $p_\infty(t) = p_0$ oscillations only occur when

$$\omega = \omega_{\mathrm{B}}, \quad \text{or} \quad \tan kA_0 = kA_0/\alpha_0, \tag{44}$$

i.e. when the exciting frequency ω experienced by each bubble is equal to the natural frequency ω_{B} of an individual bubble in an infinite liquid (bubble resonance condition) or to one of the natural frequencies ω_n of the bubble cloud. It follows from the solution of the transcendental equation (44) in the limit for low-void-fraction flows and from the expression (15) for k that the natural frequencies ω_n of the cloud are approximately given by the following sequence:

$$\omega_n^2 = \omega_{\mathrm{B}}^2 \Big/ \left(1 + \frac{3\alpha_0(1-\alpha_0) A_0^2}{(n-1/2)^2 \pi^2 R_0^2} \right); \quad n = 0, 1, 2, \ldots. \tag{45}$$

For large n this sequence converges to the frequency ω_{B} corresponding to the bubble resonance conditions. For small n the behaviour of these sequences is regulated by the values of $3\alpha_0(1-\alpha_0) A_0^2/R_0^2 = \omega_{\mathrm{B}}^2 A_0^2/c_{\mathrm{m}}^2$. When this parameter is of order unity or larger, the lower terms of the above sequence will in general extend to values much smaller than the ones given by the bubble resonance condition, thus indicating that the natural modes can occur at comparatively low frequency. On the other hand, when the reverse is the case all the terms of this sequence are contained in a small range below bubble resonance conditions. In this case all the natural modes of the system occur with a frequency only slightly lower than the bubble resonance frequency. The occurrence of resonances in the cloud divides the flow solutions in three different regimes, namely: sub-resonant ($0 < \omega < \omega_1$); trans-resonant

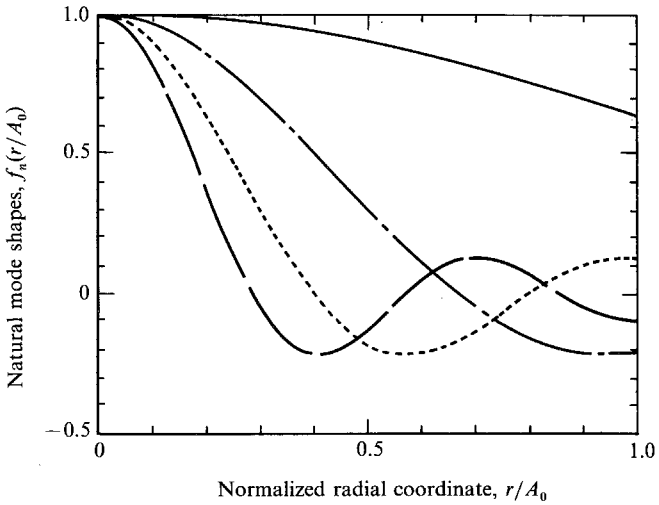

FIGURE 2. Natural mode shapes as a function of the normalized radial position r/A_0 in the cloud for various orders $n = 1$ (solid line); 2 (dash-dotted line); 3 (dotted line); 4 (broken line). The arbitrary vertical scale represents the amplitude of the normalized undamped oscillations of the bubble radius, the pressure and the bubble concentration per unit liquid volume. The oscillations of the liquid velocity and of the relative velocity between the two phases are proportional to the slopes of these curves.

($\omega_1 < \omega < \omega_B$); and super-resonant ($\omega > \omega_B$). As we shall see later, this has significant consequences on the behaviour of the flow. The above expression (45) corresponds to equation (144) of Omta (1987) for the natural frequencies of a bubble cloud. Direct comparison of these equations is not possible owing to the different modelling of bubble dynamics in the two cases. However, it is easily verified that they both reduce, as expected, to the same expression for ω_n when $3\alpha_0(1-\alpha_0)A_0^2/R_0^2 \gg 1$, when surface tension and void fraction are small and when the gas in the bubbles behaves isothermally. In this limiting case the natural frequencies of the cloud are independent of the bubble radius and vary slowly with the cloud radius and the void fraction when the total volume of the gas phase is fixed, as indicated by Omta (1987).

The natural modes of oscillation of the cloud associated to each natural frequency ω_n are easily obtained by substituting the corresponding solutions of the transcendental equation (44) in the relevant expressions of the flow parameters. The first few natural mode shapes of the relative perturbations of the bubble radius, pressure and bubble concentration are depicted in figure 2 as a function of the normalized radial coordinate r/A_0. The velocity of the liquid and the relative velocity of the two phases are proportional to the slope of these curves. Since each bubble is assumed to react to an essentially uniform far-field pressure, the validity of the model is limited to orders n such than $n \ll A_0/R_0$. Note that the first mode involves almost uniform oscillations of the bubbles at all radial positions within the cloud. Higher modes involve amplitudes of oscillation near the centre of the cloud which become larger and larger relative to the amplitudes in the rest of the cloud. In effect an outer shell of bubbles essentially shields the exterior fluid from the oscillations of the bubbles in the central core, with the result that the pressure oscillations in the exterior fluid are of smaller amplitude for the higher modes.

The relative amplitude of the undamped bubble radius oscillations at the surface

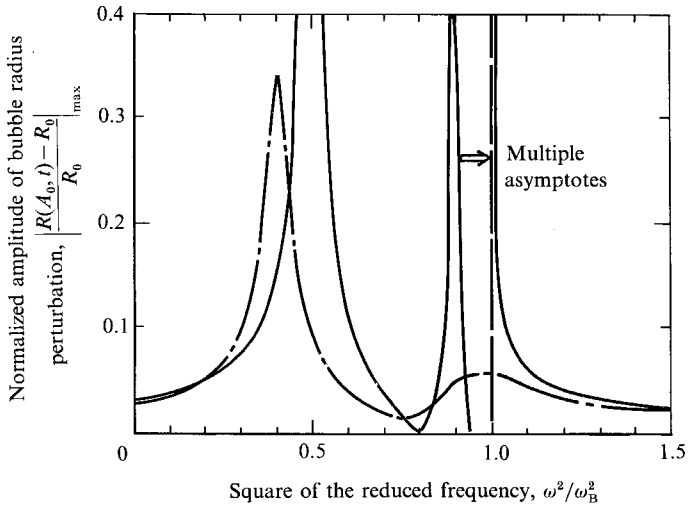

FIGURE 3. Normalized amplitude of the bubble radius oscillations at the cloud surface ($r = A_0$) as a function of the squared reduced frequency ω^2/ω_B^2 for $3\alpha_0(1-\alpha_0)A_0^2/R_0^2 = \frac{1}{4}\pi^2$ in the undamped case (solid line) and in the presence of bubble dynamics damping and relative motion (dash-dotted line).

of the cloud is shown in figure 3 as a function of the normalized square frequency for a typical case of $3\alpha_0(1-\alpha_0)A_0^2/R_0^2 = \frac{1}{4}\pi^2$. The corresponding solution with bubble dynamic damping and relative motion is also shown in the same figure for comparison. Note the peaks of the undamped bubble response at the first two natural frequencies $\omega_1^2 \approx 0.5\omega_B^2$, $\omega_2^2 \approx 0.9\omega_B^2$ and at the bubble resonance frequency. Infinitely many higher-order resonances occur between ω_2 and ω_B, but are not reported in the figure for clarity. The phase of the bubble response alternately changes by $\pm\pi$ at the location of each resonance and in correspondence with the nodes between resonances. The other flow variables also display a similar behaviour, but their higher resonance peaks are less pronounced. The introduction of energy dissipation has dramatic effects on the bubble radius response. In this case the solution, as expected, is no longer singular. More surprisingly, all resonance peaks except the first are virtually eliminated and replaced by a second much smaller and broader peak around the individual bubble natural frequency. In addition, resonance peaks are also slightly shifted toward lower frequencies. Similarly, the bubble radius response at the centre of the cloud (see figure 4) clearly shows the occurrence of the first resonant mode. The peak corresponding to the second resonant mode, whose amplitude is larger in the inner regions of the cloud, is also recognizable, although greatly attenuated. On the other hand, the peak at the bubble resonance frequency is absent because it is not associated with any global motion in the flow and because any external disturbance at the bubble natural frequency is quickly attenuated by the resonant response of the bubbles in the outer regions of the cloud. Also note that the amplitude of the bubble radius response is larger at the centre of the cloud than at the surface. The same phenomena also qualitatively characterize all of the other flow variables. Therefore the first natural mode of oscillation of the cloud at a frequency $\omega \approx \omega_1$ represents the most important component of the cloud response. Its effects also dominate the contributions of individual bubbles at their own natural frequency. These conclusions fully agree with the theory and computations of Omta (1987). The above results clearly indicate that the dynamic properties of bubble

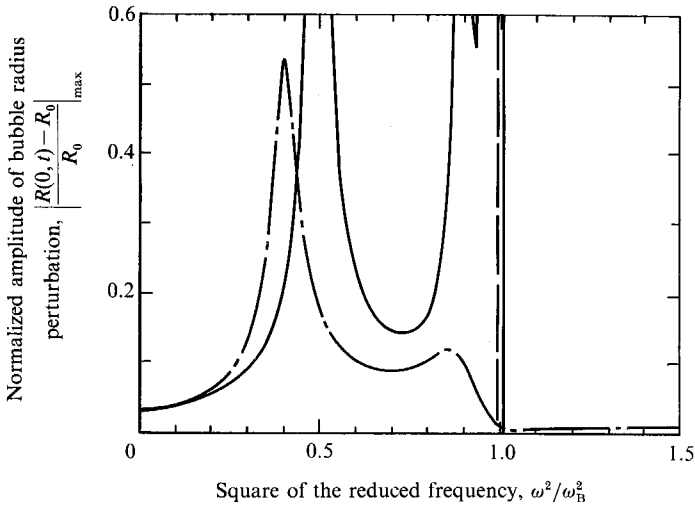

FIGURE 4. Normalized amplitude of the bubble radius oscillations at the cloud centre ($r = 0$) as a function of the squared reduced frequency ω^2/ω_B^2 for $3\alpha_0(1-\alpha_0)\,A_0^2/R_0^2 = \frac{1}{4}\pi^2$ in the undamped case (solid line) and in the presence of bubble dynamics damping and relative motion (dash-dotted line).

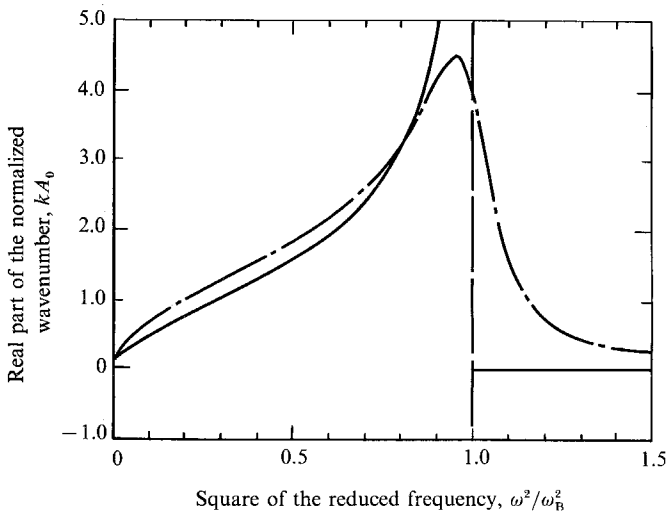

FIGURE 5. Real part of the normalized wavenumber kA_0 as a function of the squared reduced frequency ω^2/ω_B^2 for $3\alpha_0(1-\alpha_0)\,A_0^2/R_0^2 = \frac{1}{4}\pi^2$ in the undamped case (solid line) and in the presence of bubble dynamics damping and relative motion (dash-dotted line).

clouds are not adequately described in terms of the independent responses of individual bubbles, at least as long as the parameter $3\alpha_0(1-\alpha_0)\,A_0^2/R_0^2$ is of order one or larger and therefore the first natural frequency of the cloud is significantly smaller than ω_B.

The real and imaginary parts of the wavenumber k are respectively responsible for the attenuation and the speed of propagation of the radial disturbances throughout the cloud. The behaviour of kA_0 as a function of the normalized square frequency is shown in figures 5 and 6 for $3\alpha_0(1-\alpha_0)\,A_0^2/R_0^2 = \frac{1}{4}\pi^2$. Since in the no-damping case k^2 is real, k is either real or purely imaginary, with a singularity at the bubble resonance frequency. On the other hand, the introduction of bubble dynamic

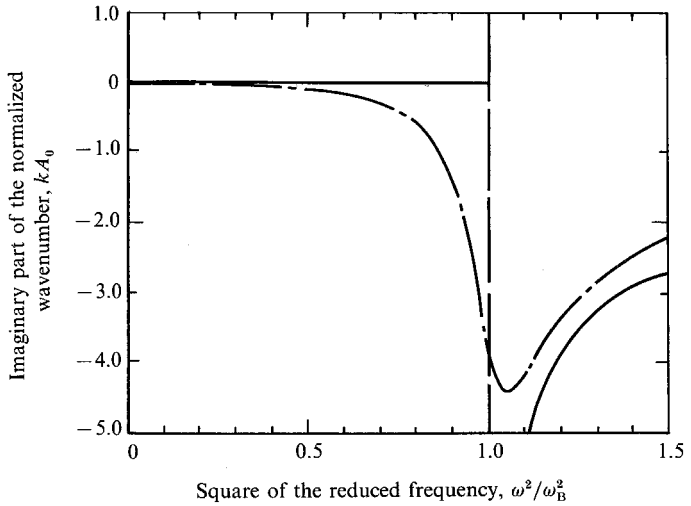

FIGURE 6. Imaginary part of the normalized wavenumber kA_0 as a function of the squared reduced frequency ω^2/ω_B^2 for $3\alpha_0(1-\alpha_0)\,A_0^2/R_0^2 = \frac{1}{4}\pi^2$ in the undamped case (solid line) and in the presence of bubble-dynamics damping and relative motion (dash-dotted line).

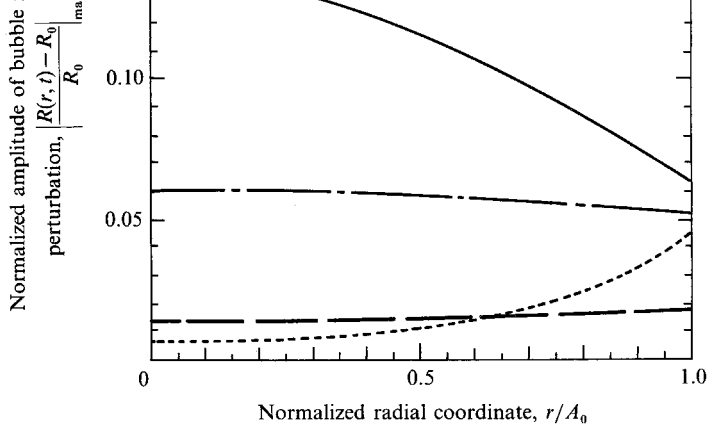

FIGURE 7. Normalized amplitude of the bubble-radius damped oscillations as a function of the normalized radial coordinate r/A_0 in the presence of bubble dynamics damping and relative motion for $3\alpha_0(1-\alpha_0)\,A_0^2/R_0^2 = \frac{1}{4}\pi^2$ and various values of the excitation frequency: $\omega^2 = \omega_1^2/2$ (solid line); $(\omega_1^2+\omega_2^2)/2$ (dash-dotted line); $1.1\omega_B^2$ (dotted line) and $2\omega_B^2$ (broken line).

damping and relative motion makes k^2 a complex number and eliminates the singularity for $\omega = \omega_B$.

The relative amplitudes of the damped bubble-radius oscillations throughout the cloud at various frequencies are illustrated in figure 7 for $3\alpha_0(1-\alpha_0)\,A_0^2/R_0^2 = \frac{1}{4}\pi^2$. Note that the bubble response is larger at the centre of the cloud for forcing frequencies below the bubble natural frequency, while the reverse is the case for super-resonant excitation. In fact, in the sub-resonant regime the bubbles have ample time to react and therefore behave in a compliant way, with the largest motion concentrated in the interior of the cloud. In this case the pressure change is essentially in phase with the

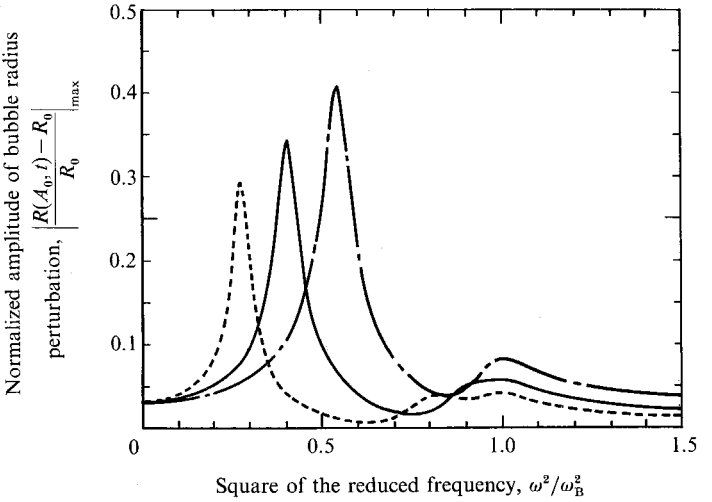

FIGURE 8. Normalized amplitude of the bubble-radius damped oscillations at the cloud surface ($r = A_0$) as a function of the squared reduced frequency ω^2/ω_B^2 at various void fractions. The curves refer to the following values of the parameter $3\alpha_0(1-\alpha_0)A_0^2/R_0^2$: $\frac{1}{4}\pi^2$ (solid line); $\frac{1}{8}\pi^2$ (dash-dotted line); and $\frac{1}{2}\pi^2$ (dotted line).

excitation and the bubble response is almost in phase opposition. Violent oscillations of the bubbles near the centre of the cloud have also been obtained by Omta (1987), in his nonlinear computations of the cloud response to a sudden change of the external pressure. In super-resonant flows, on the other hand, because of their virtual mass the bubbles cannot respond as quickly as the excitation requires and therefore appear to be 'stiffer'. This effect clearly increases with the excitation frequency and therefore the cloud response, initially more concentrated in the outer regions, becomes more uniform at higher frequencies. In this case the changes of both the pressure and of the bubble radius are almost in phase with the excitation. Finally, in the trans-resonant regime the situation is complicated by the presence of more articulated internal motions of the cloud due to the occurrence of resonances. In this case the phase of the flow parameters with respect to the excitation depends on the dominant oscillation mode in the cloud. Between the first and the second natural frequencies, for example, the bubble radius response is essentially in phase with the excitation, while the pressure is almost in phase opposition.

The effects of void-fraction changes are illustrated in figures 8–11, which show the relative amplitudes of the damped oscillations of the main flow quantities at the cloud surface as functions of the normalized square frequency for three values of the parameter $3\alpha_0(1-\alpha_0)A_0^2/R_0^2$. The corresponding bubble radius response at the centre of the cloud is illustrated in figure 12 for comparison. Since the natural frequencies are determined by the above parameter through (45), the peaks corresponding to the same natural modes of oscillation of the cloud occur at different frequencies and move towards the origin at higher void fractions. The maximum amplitudes of the liquid velocity and of the bubble concentration per unit liquid volume increase with the void fraction owing to the greater compressibility of the cloud, while the pressure peaks are not appreciably affected. On the other hand, the maximum amplitude of the bubble growth decreases with the void fraction. As mentioned in the introduction, this phenomenon has been observed by Arakeri & Shanmuganathan (1985), and by M. Billet (1986, private communication) in travelling bubble cavitating flows. It has

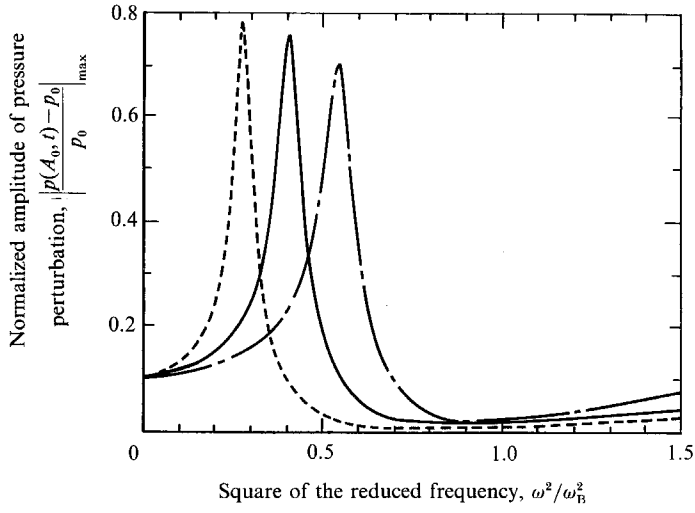

FIGURE 9. Normalized amplitude of the pressure damped oscillations at the cloud surface ($r = A_0$) as a function of the squared reduced frequency ω^2/ω_B^2 at various void fractions. Notation as figure 8.

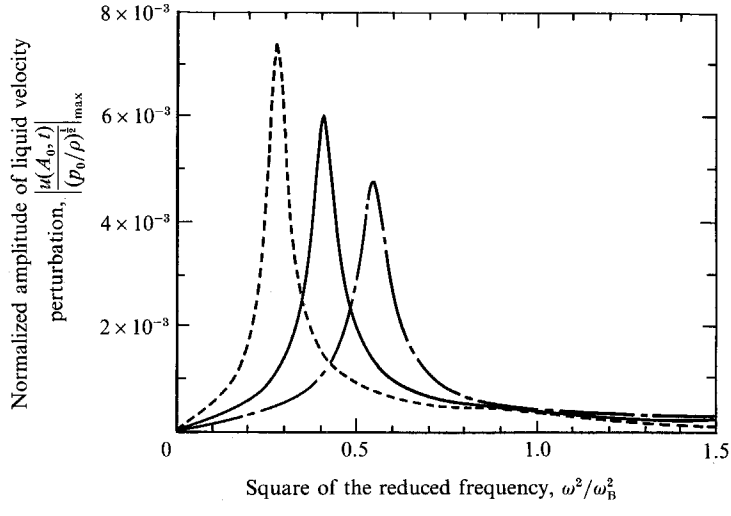

FIGURE 10. Normalized amplitude of the liquid-velocity damped oscillations at the cloud surface ($r = A_0$) as a function of the squared reduced frequency ω^2/ω_B^2 at various void fractions. Notation as figure 8.

significant consequences for the generation of noise in bubble clouds and bubbly flows in general. It also has important implications with regard to the problem of cavitation damage in cavitating flows.

Significant analogies exist between the results shown here for the case of bubble clouds subject to far-field pressure excitation and the ones previously obtained for the linearized dynamics of bubbly flows over slender surfaces (d'Agostino *et al.* 1988, 1984). In both flows the dispersive behaviour due to bubble dynamic effects is controlled by similar parameters, G and k, which depend on the void fraction and the excitation frequency. These parameters also determine the elliptic or hyperbolic nature of the problem, the penetration of external disturbances and the occurrence of the natural mode shapes and frequencies of the flow.

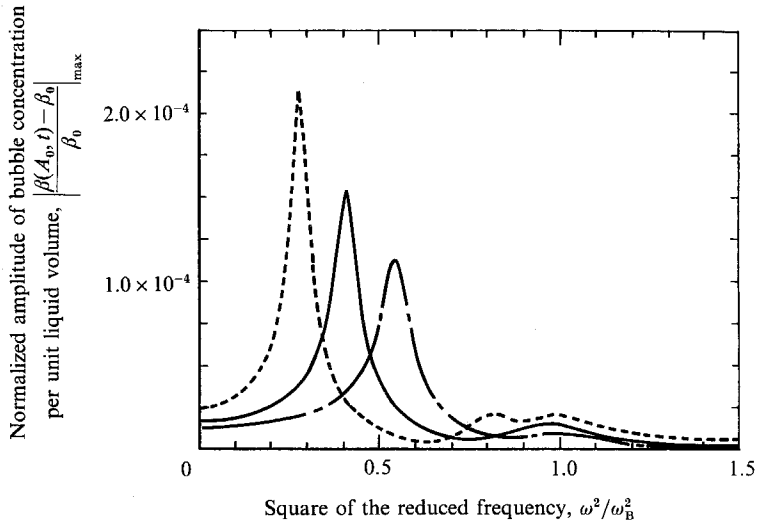

FIGURE 11. Normalized amplitude of the oscillations of the concentration of bubbles per unit liquid volume at the cloud surface ($r = A_0$) as a function of the squared reduced frequency ω^2/ω_B^2 at various void fractions. Notation as figure 8.

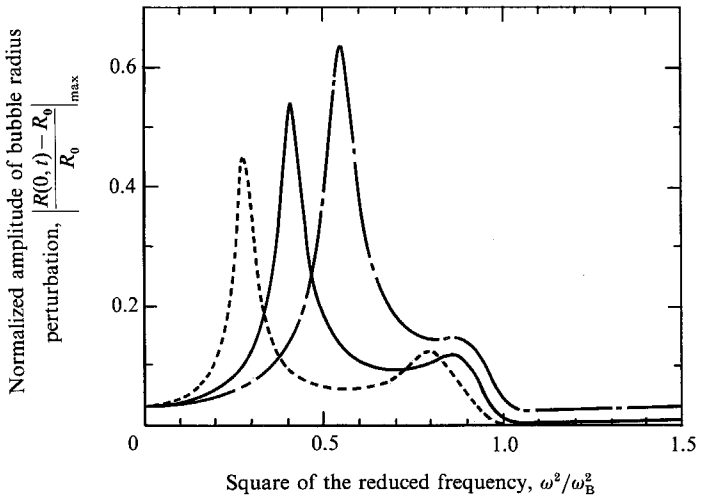

FIGURE 12. Normalized amplitude of the bubble-radius damped oscillations at the cloud centre ($r = 0$) as a function of the squared reduced frequency ω^2/ω_B^2 at various void fractions. Notation as figure 8.

We now consider a bubble cloud subject to a Gaussian-shaped far-field pressure excitation

$$p_\infty(t) = p_0[1+\eta(t)],$$

where $\eta(t) = \epsilon \exp(-t^2/2a^2)$. The Fourier transform of $\eta(t)$, as defined by (41), is

$$H(\omega) = (2/\pi)^{\frac{1}{2}}\epsilon a \exp(-\tfrac{1}{2}\omega^2 a^2).$$

As shown earlier, the solution for this flow is expressed by the inverse Fourier integrals (42). When energy dissipation is neglected the integrands in (42) have simple pole singularities corresponding to the natural mode frequencies $\omega = \omega_n$ of the

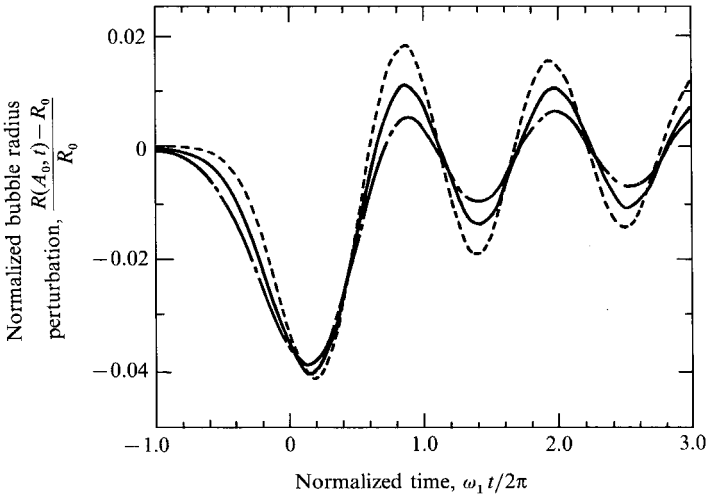

FIGURE 13. Normalized amplitude of the bubble-radius damped oscillations at the cloud surface ($r = A_0$) as a function of the normalized time $\omega_1 t/2\pi$ for $\omega_B a = \pi$ and for various void fractions. Notation as figure 8.

cloud. The bubble radius and the concentration of bubbles per unit liquid volume also have simple poles at the bubble resonance condition $\omega = \omega_B$. The latter also corresponds to the essential singularity due to the pole of k which appears in the argument of the trigonometric functions. In physical terms this reflects the fact that the absence of damping allows the bubble radius response to grow unbounded at bubble resonance conditions. This difficulty is eliminated by the introduction of dissipative effects which limit the bubble response and generate a complex k^2. In this case the singularities are removed from the real ω-axis and the integrals (42) are readily computed.

Also in the case of Gaussian-shaped excitation it is convenient to define a characteristic parameter whose value is related to the importance of cloud and bubble resonance effects. By analogy with the solution for harmonic excitation where ω is replaced by $1/a$, we choose $1/\omega_B^2 a^2$ as a representative reduced frequency parameter in the case of Gaussian-shaped excitation.

The bubble-radius normalized response as a function of time is shown in figure 13 for $\omega_B^2 a^2 = \pi^2$ and for various void fractions corresponding to three values of the parameter $3\alpha_0(1-\alpha_0)A_0^2/R_0^2$. The far-field pressure excitation has the effect of initiating an oscillatory motion in the cloud, which slowly decays owing to the presence of damping. The normalization of time with the first natural frequency ω_1 of the system clearly shows that the Gaussian-shaped change of the far-field pressure excites almost exclusively the first mode of oscillation of the bubble cloud. This finding confirms in a more general situation the observation that the first mode of oscillation represents the most important component of the cloud's dynamic response, as previously indicated by the results with harmonic excitation. Also note that the maximum amplitude of the bubble radius response increases with the void fraction. This is not surprising in view of the following considerations. In the present case the frequency spectrum of the far-field pressure excitation is mostly concentrated below the first natural frequency of the cloud. In turn, at higher values of the parameter $3\alpha_0(1-\alpha_0)A_0^2/R_0^2$ the natural frequencies of the cloud move towards the origin, thus closer to the main part of the excitation spectrum. Therefore the

transfer of energy from the external pressure field to the cloud system is enhanced, resulting in larger amplitudes of the bubble radius response at higher void fractions.

5. Limitations

We now briefly examine the restrictions imposed on the theory developed above by the various simplifying assumptions that have been made. Specifically we shall discuss the limitations due to the introduction of the continuum model of the flow, to the use of the linear perturbation approach in deriving the solution and to the neglect of the local pressure perturbations in the neighbourhood of each individual bubble. In what follows we shall refer to the solution for harmonic excitation, since it represents the basis of the generalization to arbitrary-shaped far-field forcing pressure.

The perturbation approach simply requires that $\varphi \ll 1$ in (38), a constraint that can be satisfied far from resonance conditions with proper choice of the excitation relative amplitude ϵ. This is probably the most restrictive limitation of the present analysis.

For the continuum approach to be valid, the two phases must be minutely dispersed with respect to the shortest characteristic length of the flow, here either the cloud radius A_0 or the wavelength $2\pi/k$ of the disturbances in the r-direction. Hence the average bubble spacing $s = O(R_0/\alpha_0^{\frac{1}{3}})$ is required to satisfy the most restrictive of the two conditions: $s \ll A_0$ and $ks \ll 1$.

In order to estimate the error associated with the neglect of local pressure effects due to the dynamic response of each individual bubble, we consider the pressure perturbation experienced by one bubble as a consequence of the growth or collapse of a neighbour:

$$\Delta p' = \rho\left\{\frac{R}{s}\left[R\frac{\mathrm{D}^2R}{\mathrm{D}t^2}+2\left(\frac{\mathrm{D}R}{\mathrm{D}t}\right)^2\right]-\frac{R^4}{2s^4}\left(\frac{\mathrm{D}R}{\mathrm{D}t}\right)^2\right\}, \tag{46}$$

where $R = R_0(1+\varphi)$ is given by (38). To the same order of approximation used to develop the present analysis, comparison with the global pressure change $\Delta p = p(r, t)-p_0$ expressed by (18) then shows that the local pressure perturbations are unimportant if

$$\frac{R_0}{s}\left|\frac{\omega^2(1-\mathrm{i}\omega R_0/c)}{\omega_{\mathrm{B}\omega}^2-\omega^2+\mathrm{i}\omega 2\lambda}\right| \ll 1. \tag{47}$$

Far from the bubble resonance regime, this condition is generally satisfied in low-void-fraction flows.

6. Conclusions

The results of this study reveal a number of important effects occurring in confined bubbly and cavitating flows. As anticipated in the introduction and confirmed by the present theory, the dynamics of the bubbles is strongly coupled through the pressure and velocity fields with the global dynamics of the flow in the bubble cloud. The bubbles are responsible for the occurrence of bubble resonance phenomena and for the drastic modification of the sonic speed in the medium, which decreases and becomes dispersive (frequency dependent). Furthermore, internal resonant modes of oscillation are possible at the system's natural frequencies owing to the presence of boundaries confining the bubbly region of the flow.

The inertial effects on the dynamics of the bubbles are important when the exciting frequency is comparable with or larger than the bubble natural frequency, i.e. when the reduced frequency parameters ω^2/ω_B^2, for the flows with harmonic excitation, or $1/\omega_B^2 a^2$, in the case of Gaussian-shaped excitation, are of order unity or greater. The viscous and thermal components of bubble dynamic damping are the dominant form of energy dissipation in the flow, while the contributions of the relative motion and liquid compressibility are almost always negligible in most bubbly mixtures of technical importance, regardless of the value of the other flow parameters.

The occurrence of resonances leads in turn to the identification of three different flow regimes, here indicated as sub-resonant, trans-resonant and super-resonant according to the value of the exciting frequency with respect to the cloud and the individual bubble natural frequencies. The natural frequencies of the cloud are always lower than the natural frequency of each individual bubble. In particular, they become significantly smaller than the bubble resonance frequency when the parameter $3\alpha_0(1-\alpha_0)A_0^2/R_0^2 = \omega_B^2 A_0^2/c_m^2$ is of order unity or larger. In the presence of damping the first natural mode of oscillation of the cloud is the most important component of the cloud dynamic response. Its effects dominate the ones of higher modes and also the contributions of individual bubbles at their own natural frequency. In this case significant global bubble interactions occur in the flow, with the result that the dynamic and acoustical properties of bubbly clouds are no longer adequately described in terms of the simultaneous but independent responses of the individual bubbles. In particular, as we intend to discuss in a later publication, the acoustical absorption cross-section of a bubble cloud is very significantly different from the acoustical absorption cross-section of each bubble in the cloud, as well as from that of a single larger bubble whose volume is equal to the total volume of the dispersed phase in the cloud. It appears therefore that the acoustical properties and behaviour of any given volume of the dispersed phase depend strongly on the scale of the dispersion of such phase in the bubbly mixture. This consideration should be taken into account in the analysis of noise in bubbly and cavitating flows. An increase of the void fraction also causes a substantial reduction of the amplitude of the bubble response. This, in turn, could reduce the acoustic noise in bubbly mixtures or the damage potential in cavitating flows. The above phenomena can contribute to explain some of the unexpected changes experimentally observed in the noise spectrum of bubbly cavitating flows.

The present theory has been derived under fairly restrictive simplifying assumptions involving the flow geometry and the linearization of both the velocity field and the bubble dynamics. Therefore it is not expected to provide a quantitative description of the unsteady behaviour of bubble clouds subject to far-field pressure excitation, except that in the acoustical limit. Large bubble-radius perturbations occur in most flows of practical interest; hence the most crucial limitation in the present paper is the linearization of the bubble dynamics, while the assumption of small velocity perturbations is likely to be more widely justified. If all the above linearizations were omitted, only numerical solutions could be realistically attempted. However, if only the hypothesis of linear bubble dynamics is abandoned, the development of quasi-linear theories might be possible and would have a much broader applicability.

The authors would like to thank Cecilia Lin for her help in drawing the pictures and Steve Ceccio for his help in carrying out some of the computations. This work was supported by the Naval Sea System Command General Hydromechanics

Research Program Administered by the David Taylor Naval Ship Research and Development Center under Contract No. N00167-85-K-0165, by the Office of Naval Research under contract No. N0014-83-K-0506 and by a Fellowship for Technological Research administered by the North Atlantic Treaty Organization – Consiglio Nazionale delle Ricerche, Italy, Competition No. 215.15/11 of 11.5.1982. Their support is gratefully acknowledged.

REFERENCES

ARAKERI, V. H. & SHANMUGANATHAN, V. 1985 On the evidence for the effect of bubble interference on cavitation noise. *J. Fluid Mech.* **159**, 131–150.

BIESHEUVEL, A. & VAN WIJNGAARDEN, L. 1984 Two phase flow equations for a dilute dispersion of gas bubbles in liquid. *J. Fluid Mech.* **148**, 301–318.

CARSTENSEN, E. L. & FOLDY, L. L. 1947 Propagation of sound through a liquid containing bubbles. *J. Acoust. Soc. Am.* **19**, 481–501.

CHAHINE, G. L. 1982*a* Pressure field generated by the collective collapse of cavitation bubbles. *IAHR Symp. on Operating Problems of Pump Stations and Power Plants, Amsterdam, Netherlands*, Vol. 1, Paper 2.

CHAHINE, G. L. 1982*b* Cloud cavitation theory. *14th Symp. on Naval Hydrodynamics, August 1982*, Session I, p. 51.

D'AGOSTINO, L. & BRENNEN, C. E. 1983 On the acoustical dynamics of bubble clouds. *ASME Cavitation and Multiphase Flow Forum*, pp. 72–75.

D'AGOSTINO, L., BRENNEN, C. E. & ACOSTA, A. J. 1984 On the linearized dynamics of two-dimensional bubbly flows over wave-shaped surfaces. *ASME Cavitation and Multiphase Flow Forum*, pp. 8–13.

D'AGOSTINO, L., BRENNEN, C. E. & ACOSTA, A. J. 1988 Linearized dynamics of two-dimensional bubbly and cavitating flows over slender surfaces. *J. Fluid Mech.* **192**, 485–509.

FOLDY, L. L. 1945 The multiple scattering of waves. *Phys. Rev.* **67**, 107–119.

FOX, S. E., CURLEY, S. R. & LARSON, G. S. 1955 Phase velocity and absorption measurements in water containing air bubbles. *J. Acoust. Soc. Am.* **27**, 534–539.

ISHII, M. 1975 *Thermo-Fluid Dynamic Theory of Two-Phase Flow.* Eyrolles.

KNAPP, R. T., DAILY, J. W. & HAMMIT, F. G. 1970 *Cavitation.* McGraw Hill.

MACPHERSON, J. D. 1957 The effect of gas bubbles on sound propagation in water. *Proc. Phys. Soc. Lond.* B**70**, 85–92.

MARBOE, R. C., BILLET, M. L. & THOMPSON, D. E. 1986 Some aspects of traveling bubble cavitation and noise. *Intl Symp. on Cavitation and Multiphase Flow Noise, Anaheim, California.*

MØRCH, K. A. 1980 On the collapse of cavity cluster in flow cavitation. *Proc. 1st Intl Conf. on Cavitation and Inhomogeneities in Underwater Acoustics.* Springer Series in Electrophysics, Vol 4, pp. 95–100. Springer.

MØRCH, K. A. 1981 Cavity cluster dynamics and cavitation erosion. *ASME Cavitation and Polyphase Flow Forum*, pp. 1–10.

MØRCH, K. A. 1982 Energy considerations on the collapse of cavity cluster. *Appl. Sci. Res.* **38**, 313.

MUIR, T. F. & EICHHORN, R. 1963 Compressible flow of an air–water mixture through a vertical two-dimensional converging-diverging nozzle. *Proc. Heat Trans., Fluid Mech. Inst., Stanford.* Stanford University Press.

NOORDZIJ, L. 1973 Shock waves in mixtures of liquids and air bubbles. Doctoral thesis, Technische Hogeschool, Twente, Netherlands.

NOORDZIJ, L. & WIJNGAARDEN, L. VAN 1974 Relaxation effects, caused by relative motion, on shock waves in gas-bubble/liquid mixtures. *J. Fluid Mech.* **66**, 115–143.

OMTA, R. 1987 Oscillations of a cloud of bubbles of small and not so small amplitude. *J. Acoust. Soc. Am.* **82**, 1018–1033.

PLESSET, M. S. & PROSPERETTI, A. 1977 Bubble dynamics and cavitation. *Ann. Rev. Fluid. Mech.* **9**, 145–185.

PROSPERETTI, A. 1984 Bubble phenomena in sound fields: part one. *Ultrasonics*, March, 69–78.

PYLKKÄNEN, J. V. 1986 Characteristics of spherical cloud cavity. *Advancements in Aerodynamics, Fluid Mechanics and Hydraulics* (ed. R. Arndt *et al.*), ASCE Conference, Minneapolis, Minnesota, pp. 96–103.

SILBERMAN, E. 1957 Sound velocity and attenuation in bubbly mixtures measured in standing wave tubes. *J. Acoust. Soc. Am.* **18**, 925–933.

STEWART, H. B. & WENDROFF, B. 1984 Two-phase flows: models and methods. *J. Comput. Phys.* **56**, 363–409.

TANGREN, R. F., DODGE, C. H. & SEIFERT, H. S. 1949 Compressibility effects in two-phase flows. *J. Appl. Phys.* **20**, 637–645.

VOINOV, O. V. 1973 Force acting on a sphere in an inhomogeneous flow of an ideal incompressible fluid. Plenum (transl. from *Zhurnal Prikladnoi Mekhaniki i Tekhnicheskoi Fiziki*, No. 4, pp. 182–184, July–August 1973).

WIJNGAARDEN, L. VAN 1964 On the collective collapse of a large number of gas bubbles in water. *Proc. 11th Intl Cong. Appl. Mech.*, pp. 854–861. Springer.

WIJNGAARDEN, L. VAN 1968 On the equations of motion of mixtures of liquid and gas bubbles. *J. Fluid Mech.* **33**, 465–474.

WIJNGAARDEN, L. VAN 1972 One-dimensional flow of liquids containing small gas bubbles. *Ann. Rev. Fluid Mech.* **4**, 369–396.

WIJNGAARDEN, L. VAN 1980 Sound and shock waves in bubbly liquids. In *Cavitation and Inhomogeneities in Underwater Acoustics* (ed. W. Lauterborn), pp. 127–140. Springler.